

Ordering and correlation of cluster orientations in CaCd_6

PETER BROMMER[†], FRANZ GÄHLER^{*†} and MAREK MIHALKOVIČ[‡]

[†]Institut für Theoretische und Angewandte Physik, Universität Stuttgart, 70550 Stuttgart, Germany

[‡]Institute of Physics, Slovak Academy of Sciences, 84511 Bratislava, Slovakia

(Received 00 Month 200x; in final form 00 Month 200x)

In order to study the low temperature phase transition in CaCd_6 , which is attributed to a reordering of the innermost tetrahedral cluster shells, accurate Embedded-Atom-Method potentials are developed for this system. With these potentials, the ideal cluster structure and the couplings between neighbouring clusters are determined. From these data, an effective hamiltonian for the cluster orientations is derived. The hamiltonian is used in Monte Carlo simulations, which exhibit a sharp jump in the internal energy near the expected transition temperature.

1 Introduction

The thermodynamically stable binary quasicrystals in the Ca-Cd and Yb-Cd systems [1, 2] as well as many of their periodic approximants can be understood as packings of essentially identical clusters, plus some extra glue atoms between the clusters [3, 4]. In particular, the cubic 1/1-approximants can be regarded as bcc-packings of the clusters, which contain a total of 66 atoms arranged in four shells. Whereas the outer three shells are icosahedrally symmetric, the innermost shell is believed to consist of four atoms at the corners of a heavily deformed tetrahedron [5].

The cubic 1/1-approximants CaCd_6 and YbCd_6 exhibit an order-disorder phase transition at 100 K and 110 K, respectively, which is attributed to a reordering or disordering of the orientations of the innermost tetrahedral shells of the clusters, and which is visible as a peak in the heat capacity, and a discontinuity of the resistivity [6, 7]. The precise structure of the innermost cluster shell, and especially the nature of their ordering, is still largely unclear. From X-ray diffraction, Gómez and Lidin [5] have derived a distorted tetrahedron for the innermost shell, which is clearly better than a regular tetrahedron, but which may not be the final answer yet. Based on this proposal, Nozawa and Ishii [8, 9] have computed with ab-initio methods the energies of structures with different tetrahedron shapes and orientations, and performed also some relaxation simulations. These methods are computationally very demanding, however, and it is not feasible to perform such simulations for large supercells.

Ab-initio simulations can therefore not directly be used for analysing the order-disorder phase transition. Such systems sizes are accessible only with classical simulations, which still must provide nearly ab-initio precision, however. We show in this paper that sufficiently accurate potentials of Embedded-Atom-Method (EAM) [10] or glue type [11] can indeed be determined, by fitting them to reproduce ab-initio derived forces and energies of carefully selected reference structures. With such potentials, we analyse the ideal cluster structure, including the innermost tetrahedron shell and the induced deformation of the outer shells, as well as the coupling between the orientations of neighbouring clusters through the deformations of the outer shells.

Classical atomistic simulations are still too slow to analyse the details of the phase transition, however. For this purpose, we derive in a second step an effective hamiltonian for the couplings between the different cluster orientations, whose parameters are determined by fitting to energies computed with EAM potentials. This hamiltonian is used in Monte Carlo simulations, which indeed exhibit a phase transition near the expected temperature.

*Corresponding author. Email: gaehler@itap.physik.uni-stuttgart.de

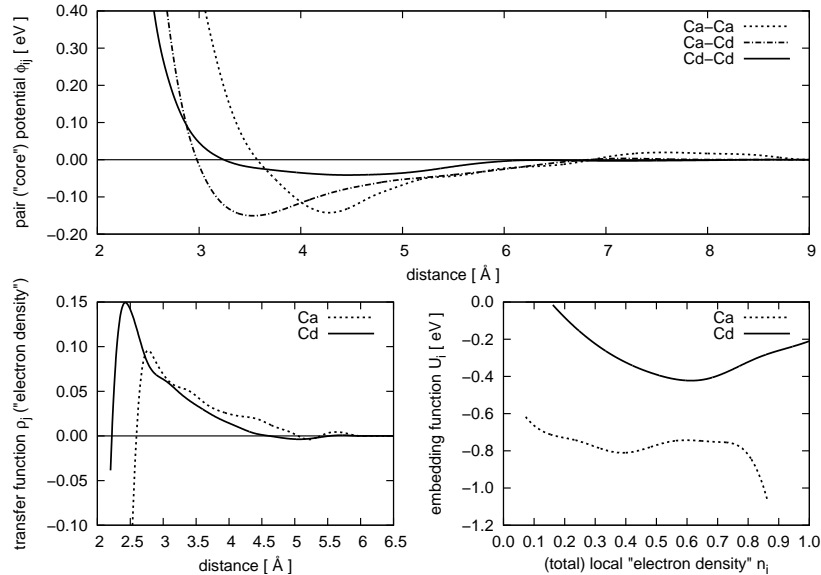


Figure 1. Potential functions of the Ca-Cd EAM potential.

2 Effective potentials from ab-initio data

We have shown [12] that classical potentials of EAM [10] or glue type [11] can accurately model the interactions in several complex intermetallic alloys, among them icosahedral Ca-Cd quasicrystals and their periodic approximants. EAM potentials, which take the functional form

$$V = \sum_{i,j < i} \phi_{ij}(r_{ij}) + \sum_i U_i(n_i), \quad \text{with} \quad n_i = \sum_{j \neq i} \rho_j(r_{ij}), \quad (1)$$

consist of a pair potential term and a (many-body) embedding term depending on a local density n_i , which in turn is determined by contributions ρ_j of the neighbouring atoms. For maximal flexibility, the functions ϕ , ρ , and U are represented by tabulated values and spline interpolation. The tabulated values are the potential parameters, which are determined by fitting the potential to reproduce ab-initio computed forces, energies, and stresses of carefully selected reference configurations. This procedure is called force matching [11]. The details of our implementation are explained in [13].

The capabilities of the generated potential are determined by the collection of reference structures used in the fit. For the present purpose, we have selected the smaller canonical cell approximants [3,4] listed in Table 1 of [4] (those with up to 168 atoms), along with the hexagonal phase with Pearson symbol hP68. All these structures have been taken from the alloy database [14]. The canonical cell approximants represent different packings of the same cluster as the 1/1-approximant (which itself consists of decorated canonical A cells). Besides these perfect structures, also expanded and compressed variants were created, as well as snapshots at various temperatures from 200 K to 700 K. The latter were produced with molecular dynamics (MD) simulations using an ad-hoc pair potential, and serve to introduce deviations of the atoms from their ideal positions. For all these structures, 19 configurations in total, the individual forces on all atoms and total energies and stresses were computed ab-initio, using the VASP program [15,16] in generalized gradient approximation (GGA) and with the Projector Augmented Wave (PAW) method [17,18]. We confined ourselves to the Ca-Cd case, as Ca is much better behaved in ab-initio simulations, compared to Yb. With these reference data, a first EAM potential was fitted, which was used to produce better MD snapshots of the 1/1-approximant. In this way, 15 further configurations were added to the reference configurations, and the fit was repeated to obtain the final potential. The potential functions are displayed in Fig. 1. Note that they do not show any noticeable Friedel oscillations, in contrast to the potential for decagonal Al-Ni-Co [12].

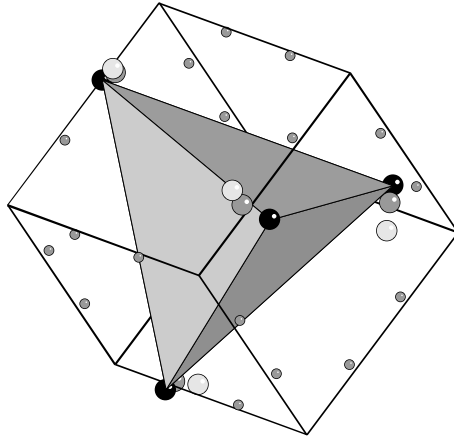


Figure 2. Ideal tetrahedron, compared to Gómez-Lidin tetrahedron. The corners of the Gómez-Lidin tetrahedron (large medium gray dots) relax to new positions (black dots). The light gray dots are corners of other relaxed tetrahedra, so that the total number of possible tetrahedron corners is doubled. Shown are also the other Gómez-Lidin tetrahedron corners as smaller medium gray dots. The cube is drawn as a guide to the eye.

3 Molecular dynamics simulations

As a first application, we have studied the stability of the Gómez-Lidin tetrahedra [5] as innermost shells. We have generated all possible combinations of orientations of the tetrahedra in a cubic cell with two clusters, and relaxed these structures to the nearest energy minimum. The resulting relaxed structures had six different energies in total, differing maximally by 0.17 meV/atom. The relaxed tetrahedra were all identical (up to symmetry), the energy difference coming from the different relative orientations of the two tetrahedra. This ideal tetrahedron is not equal to the Gómez-Lidin one, however. Each tetrahedron atom relaxes in a specific way without further symmetry breaking, so that the total number of distinct tetrahedra remains 12, like the number of Gómez-Lidin tetrahedra. The total number of possible corner positions has doubled, however (Fig. 2). For instance, the Cd1b position at $(0.0268, 0.0806, 0.0764)$ [5] moves to either $(0.0244, 0.0899, 0.0697)$ or $(0.0244, 0.0697, 0.0899)$, by 0.17\AA or 0.29\AA , respectively, where the new positions are chosen such that the two short tetrahedron edges get longer at each end. Our relaxation simulations also show that the surrounding shells of the clusters are strongly deformed by the inner tetrahedron. The stability of the ideal cluster has been verified also with ab-initio relaxations.

In a second step, finite temperature MD simulations were performed with a larger sample, consisting of $5 \times 5 \times 5$ cubic unit cells (250 clusters). These simulations show that, starting from an ordered low-temperature state, the tetrahedron orientations start to change at around 100 K, and even a few non-ideal tetrahedra show up. It was not possible, however, to see any clear sign of the expected phase transition, like a peak in the heat capacity. We suspect that the time scale accessible in MD is too short to sample phase space sufficiently well to see the phase transition. A further step in our modelling of the interactions is therefore required.

4 Effective cluster hamiltonian

In order to obtain better statistics, we need to reduce the degrees of freedom. All clusters in low temperature states apparently have the same innermost shells in the form of the ideal tetrahedron introduced above, which occurs in twelve different orientations. We therefore confine ourselves to such configurations, for which we set up an effective hamiltonian modelling the interactions between neighbouring clusters via induced deformations of the outer shells. Neighbouring clusters can be in contact along two-fold or three-fold directions. Taking into account the different orientations of the inner tetrahedra at both ends of a bond, there are, up to symmetry, 26 types of 2-fold bonds and 16 types of 3-fold bonds. We assume that each bond of type α contributes an energy E_α to the hamiltonian.

In order to determine the energies E_α , 9394 supercell configurations with up to 64 clusters containing randomly oriented ideal tetrahedra were generated and relaxed to their ground state, using the EAM

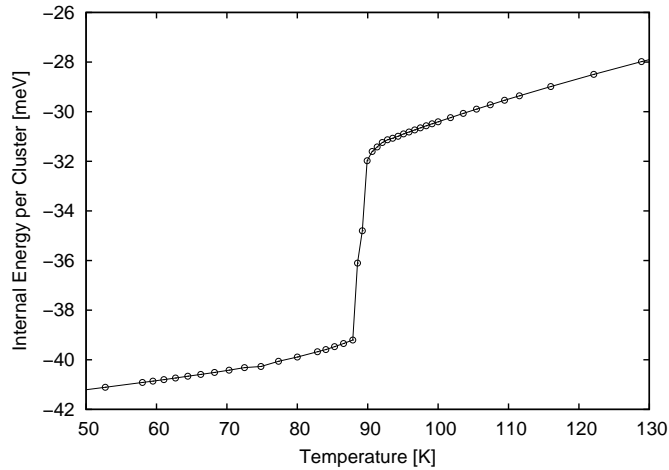


Figure 3. Internal energy as a function of temperature for the effective cluster hamiltonian. A sharp jump is displayed at about 89 K.

potentials. For each of the relaxed configurations, the total energy and the bond frequencies were measured. As the initial structures consisted of clusters with undeformed outer shells, with only the inner tetrahedra replaced, the relaxation is performed in two steps. In a first step, the tetrahedron atoms (already in almost ideal position) were held fixed, so that the deformation of the surrounding shells could develop. Only in a second step, a final relaxation with all atoms mobile was performed. The energies E_α were then determined in a least-square fit, resulting in a RMS deviation of about 1.7 meV per cluster, which is 3% of the width of the spectrum.

The cluster hamiltonian so derived can now be used in extensive Monte Carlo simulations. With a sample of $4 \times 4 \times 4$ unit cells containing 128 clusters, we have determined the internal energy as a function of temperature, which shows a sharp jump at about 89 K (Fig. 3), not far from the experimental transition temperature of 100 K [7]. This energy jump ΔE corresponds to any entropy jump $\Delta E/k_B T_0$ of roughly $1k_B$ per cluster, which is about twice the amount estimated in [6].

By simulated annealing, it should also be possible to determine the order in the low-temperature state, and the nature of the disordering at the transition. All we can say at the moment, however, is that the ground state might be a complicated superstructure (compare also [19]) not easy to reach in cooling simulations. Further work is required here.

5 Discussion

With our EAM potentials, the interaction between the inner tetrahedra of neighbouring clusters is mediated essentially via induced deformations of the outer shells. The range of the potentials (9Å) is actually shorter than the distance between neighbouring tetrahedra. In ab-initio simulations, Nozawa and Ishii [8] have observed a direct tetrahedron-tetrahedron interaction with undeformed outer shells. These direct coupling energies are largely overshadowed, however, by the strong relaxation of the outer shells, which leads to energy differences at least 20 times larger. It remains therefore unclear whether long-range terms are really significant. Our results show that the phase transition temperature at least is reasonably reproduced also without including long-range terms in the potentials.

Our MD simulations show that the low-temperature structures up to and beyond the phase transition essentially consist of ideal tetrahedra in different orientations. Only few non-ideal tetrahedra have shown up in the simulations. What changes in the phase transition is the kind of (superlattice) ordering of the ideal tetrahedra, not the nature of the tetrahedra themselves. The energy difference between ideal and non-ideal tetrahedra is therefore not relevant for the transition temperature.

6 Conclusion

We have shown that classical EAM potentials can accurately model the interactions in complex Ca-Cd alloys, notably the cubic 1/1-approximant CaCd_6 . Due to the selection of reference structures to which they were fitted, the potentials are particularly suitable for the assessment and relaxation of ground-state like, low-temperature structures. This makes them very promising for the structure optimisation of large unit cell approximants, which are packings of the same clusters as the presently studied 1/1-approximant. With such large unit cells, ab-initio methods definitely reach their limit, whereas simulations with classical potentials are still extremely fast.

Nevertheless, for the study of structural phase transitions MD is not the ideal tool. For this purpose, we have derived from the EAM potentials an effective hamiltonian for a restricted subset of low-temperature configurations, with which the order-disorder phase transition can now be studied in detail. The precise cluster ordering in the low-temperature state still needs to be determined, but the transition temperature is reproduced already reasonably accurately.

Acknowledgement

This work was funded by the Deutsche Forschungsgemeinschaft through Sonderforschungsbereich 382. MM also acknowledges support by Grant Agencies for Science of Slovakia, grant nos. VEGA 2/5096/25 and APVT-51052702.

References

- [1] J. Q. Guo, E. Abe and A. P. Tsai. Phys. Rev. B **62** R14605 (2000).
- [2] A. P. Tsai, J. Q. Guo, E. Abe *et al.* Nature **408** 537 (2000).
- [3] M. Widom and M. Mihalkovič. Mat. Res. Soc. Symp. Proc. **805** LL1.10.1 LL1.10.6 (2004).
- [4] M. Mihalkovič and M. Widom. Phil. Mag. **86** 519 (2006).
- [5] C. P. Gómez and S. Lidin. Phys. Rev. B **68** 024203 (2003).
- [6] R. Tamura, K. Edagawa, C. Aoki *et al.* Phys. Rev. B **68** 174105 (2003).
- [7] R. Tamura, K. Edagawa, Y. Murao *et al.* J. Non-Cryst. Solids **334&335** 173 (2004).
- [8] K. Nozawa and Y. Ishii. *First-Principles Calculations for Structures of Cubic Approximant Cd_6Ca* , preprint (2005).
- [9] K. Nozawa and Y. Ishii. Phil. Mag. **86** 615 (2006).
- [10] M. S. Daw, S. M. Foiles and M. I. Baskes. Mater. Sci. Rep. **9** 251 (1993).
- [11] F. Ercolessi and J. B. Adams. Europhys. Lett. **26** 583 (1994).
- [12] P. Brommer and F. Gähler. Phil. Mag. **86** 753 (2006).
- [13] P. Brommer and F. Gähler. *Potfit: effective potentials from ab-initio data*, preprint (2006).
- [14] M. Widom and M. Mihalkovič. Alloy database, available online at <http://alloy.phys.cmu.edu> (accessed 31 August 2006).
- [15] G. Kresse and J. Hafner. Phys. Rev. B **47** 558 (1993).
- [16] G. Kresse and J. Furthmüller. Phys. Rev. B **54** 11169 (1996).
- [17] P. E. Blöchl. Phys. Rev. B **50** 17953 (1994).
- [18] G. Kresse and D. Joubert. Phys. Rev. B **59** 1758 (1999).
- [19] R. Tamura, K. Edagawa, K. Shibata *et al.* Phys. Rev. B **72** 174211 (2005).